ViO-Com: Feed-Forward Compensation Using Vision-Based Optimization for High-Precision Surgical Manipulation

DongHoon Baek, Young-Hoon Nho, and Dong-Soo Kwon, *Senior Member, IEEE*

***Abstract*—Tendon-sheath mechanisms offer a means for a flexible surgical robot to be operated efficiently in restricted environments, for example, the long and narrow paths inside human organs. However, nonlinear hysteresis interferes with the precise motion control of a flexible robot. Generally, the characteristics of hysteresis can change due to changes in cable-related effects and robot shapes, which increase the difficulty associated with achieving precise control of surgical robots. Although several methods have been proposed to solve this problem, most of these methods offer limited performance and are unstable in realistic situations. In this letter, we present a vision-based optimized feedforward compensation (ViO-Com) scheme for a cable-driven surgical robot that reduces hysteresis as a practical approach, regardless of any unmeasured hysteresis while maintaining stable motion. A CycleGAN and a Siamese CNN were used to estimate the actual joint angle of a surgical manipulator, and the Bouc–Wen model with optimized parameters was used for feed-forward compensation. The results obtained using a real surgical robot platform K-FLEX suggest that the performance of ViO-Com is superior to that of vision-based feedback compensation under various hysteresis condition, and its accuracy is improved by 67%.**

***Index Terms*—AI-based methods, machine learning for robot control, medical robots and systems.**

I. INTRODUCTION

FLEXIBLE cable-driven surgical robots are expected to be the future of robotic surgery owing to their suitability for use in minimally invasive surgery, such as their high transmission power, dexterity, and flexibility [1], [2]. With these advantages, flexible surgical robots can access clinical targets along long, narrow, and tortuous paths without the need for making any abdominal incisions in the human body.

Most surgical robots are based on tendon-sheath mechanisms (TSMs) that can transmit mechanical power from an actuator to the distal joint of a surgical manipulator located at a remote site through a flexible insertion tube [1], [2]. This mechanism consists of a hollow coiled wire (sheath) and an internal cable (tendon), and it helps to operate a surgical robot by transmitting force/motion in extremely constrained and compact spaces. Moreover, a high-power electrical actuator is not required at the distal end to move a surgical manipulator.

Although it is preferrable to use TSMs in many cable-driven surgical robots, the hysteresis caused by nonlinear friction, backlash, and cable-related effects (e.g., wire elongation, wire slack, and buckling) degrades the control accuracy of a surgical manipulator [3]. In addition, it is not possible to attach additional sensors at the surgical manipulator due to their size and the sterilization compliance requirements of medical devices. Even though surgeons are able to use visual feedback during robotic surgery, their surgical performance might decrease, especially in complex sites with large hysteresis, where the robot shape is significantly deformed [4].

Many studies have been conducted to autonomously increase the control accuracy of cable-driven surgical robots. Although some of them are able to be implemented in real surgery, to the best of our knowledge, there is no existing solution to achieve high-precision surgical manipulation in a stable and practical manner when faced with diverse and unknown sheath configurations.

In the present work, as a practical solution, we propose a vision-based optimized feed-forward compensation scheme (ViO-Com) that uses a Bouc–Wen hysteresis model with optimized parameters identified by using only an endoscopic camera. The method requires only a simple calibration scheme that is commonly performed in many robots before they are operated, ViO-Com offers more effective compensation performance in comparison to the feedback approach without any manual parameter tuning while ensuring control stability even with unknown and unmeasured robot shapes. This strategy is performed offline before starting operation and make use of fixed optimized parameter during surgery.

The contributions of this work are as follows: (1) ViO-Com, a new pipeline is proposed for the hysteresis compensation

Manuscript received June 13, 2021; accepted October 13, 2021. Date of publication October 27, 2021; date of current version November 11, 2021. This letter was recommended for publication by Associate Editor Rudolph Triebel and Editor Markus Vincze upon evaluation of the reviewers' comments. This work was supported in part by the International Joint Technology Development Project funded by the Korean Ministry of Trade, Industry and Energy under Grant P0006718 and in part by EasyEndo Surgical Inc. *(DongHoon Baek and Young-Hoon Nho contributed equally to this work.) (Corresponding author: Dong-Soo Kwon.)*

DongHoon Baek is with the Department of Mechanical Science and Engineering, University of Illinois Urbana-Champaign, Champaign, IL 61820 USA, and was also with EasyEndo Surgical Inc., Daejeon 34051, South Korea (e-mail: dbaek4@illinois.edu).

Young-Hoon Nho is with the Department of Neurosurgery, University of Pennsylvania, Philadelphia, PA 19104 USA, and was also with the EasyEndo Surgical Inc., Daejeon 34051, South Korea (e-mail: younghoon.nho@pennmedicine.upenn.edu).

Dong-Soo Kwon is with the EasyEndo Surgical Inc., Daejeon 34051, South Korea, and also with the Department of Mechanical Engineering, Korea Advanced Institute of Science and Technology, Daejeon 34141, South Korea (e-mail: kwonds@kaist.ac.kr).

This letter has supplementary downloadable material available at https://doi.org/10.1109/LRA.2021.3123375, provided by the authors.

Digital Object Identifier 10.1109/LRA.2021.3123375

of cable-driven flexible robots that can enhance their surgical manipulation abilities practically without any prior knowledge of the present robot shape or the use of external sensors. (2) Experimental results indicate that ViO-Com considerably outperforms the current state-of-the-art vision-based feedback compensator in terms of accuracy while offering superior control stability. (3) In the process of suggesting the most appropriate method, 10 different optimization methods are evaluated and analyzed to rapidly identify the parameters of the Bouc–Wen model with high accuracy and success rate. (4) ViO-Com has potential for use in other surgical robots, as indicated by the results of an experiment involving the robot K-FLEX, because it enhances control performance.

II. RELATED WORK

Literature for addressing the hysteresis of the TSM can be grouped into two categories depending on whether the underlying methods use external sensors during robot operation: offline methods and online methods.

Offline methods are based on static models that do not change during a surgical operation (e.g., model-based feedforward compensation, learning kinematic model, and calibration technique). Many mathematical models and suitable control strategies have been proposed to mitigate the effects of hysteresis. The Bouc–Wen model and the Prandtl–Ishlinskii model that can reflect dynamic characteristics are widely used in the robotics field and they are implemented after the parameter optimization process [5], [6]. Do *et al.* [6] introduced a novel backlash hysteresis model based on the Bouc–Wen model and an inverse control scheme to enhance the control accuracy of a single TSM, but this model is limited only to a fixed sheath configuration of the TSM. In a later study, they proposed an adaptive control scheme and compared it to a direct Bouc–Wen-model-based feedforward compensation scheme [7]. Although the adaptive method was able to reduce the hysteresis due to changes in the tendon-sheath configuration, the evaluation was performed under several impractical assumptions. Jung *et al.* [8] introduced a feedforward torque control scheme with a double tendon-sheath actuation mechanism and applied it to a multiple-degrees-of-freedom (DoFs) system. However, the performance of this scheme deteriorated when the moving direction of the tendon was changed. Recently, with the advent of deep learning, several data-driven methods for learning the inverse kinematics of TSMs have been proposed [9]–[11]. These can describe the hysteresis without using any mathematical model but has still limitation in an environment with unknown hysteresis. Lee *et al.* [12] proposed a hysteresis model to simultaneously compensate for backlash and dead zone. Although this method used a practical approach to identify the model parameters by using the motor current during the calibration step, it could not compensate for the influence of changes in the sheath shape.

In spite of their many advantages, the accuracy of offline methods can easily decrease when a prior hysteresis change occurs because of reasons such as a deformation of sheath configuration and change in instrument (surgical manipulator). Moreover, to identify the parameters of a mathematical model (e.g., Bouc–Wen model), the use of an external sensor is necessary. Because it is difficult to recognize the current sheath configuration of a flexible surgical robot in actual surgery, a more robust and practical approach is required.

To cope with the uncertainties and dynamic disturbances encountered in surgical environments, online methods that use closed-loop controllers with feedback information have been proposed. Electromagnetic position sensors have been used to measure the pose of a surgical manipulator [13], but it is difficult to integrate these sensors into actual surgical applications because of sterilization-related issues. Several pose estimation algorithms using a camera have been claimed as well [14]–[16]. Even though these are presented their performance in *ex-vivo* condition, they focused on and experimented for pose estimation rather than hysteresis reduction. Some researchers have been tried to alleviate hysteresis using vision-based estimator [17]–[20]. These methods offer more robust control performance than offline methods when the prior hysteresis changes. However, considering the nature of these methods, changes in illumination (e.g., a change of light) and occlusion can degrade their performance. Baek *et al.* proposed a feedback compensator on the basis of a learning-based hybrid estimator. This compensator reduced hysteresis even under the simultaneous occurrence of occlusion and sheath deformation [21]. However, its control performance was unstable in an intricate situation involving inevitable occlusion.

III. METHOD

The overall pipeline of the proposed ViO-Com method is based on the executed sequence illustrated in Fig. 2. First, generative adversarial network (GAN)-based surgical manipulator segmentation is performed to obtain a binary segmented image. Next, we acquire a data sequence, including estimated joint angles, by calibrating the robot. Finally, the parameters of the Bouc–Wen model are identified using the optimization method, and are applied to the feedforward controller. Overall implementation codes can be accessible via https://github.com/nhoyh/hysteresis_compensation_ROS.

A. Flexible Surgical Robot, K-FLEX

A cable-driven surgical robot K-FLEX [1] was utilized to validate the performance of ViO-Com (Fig. 1). The system consisted of a fixed 2D RGB camera with 1920×1080 resolution (MD-V31105L-77, MISUMI, Taiwan), a four-DoF surgical manipulator (translation d, rotation θ_1, yaw θ_2, and pitch θ_3), and a flexible tube. The manipulator was driven using a TSM and controlled using inverse kinematics with the same of the previous work [21]. For measuring the actual joint angle of the manipulator θ_a, an Aurora sensor (Northern Digital Inc., Canada) was used. To be less affected by the metal material, we used a plastic holder made of a rapid prototype. All developed software was integrated using Robot Operating System (ROS). The desired input was given through the graphic user interface.

B. Surgical Manipulator Segmentation using Generative Adversarial Network

The surgical tool segmentation was addressed to reduce the variance from diverse surgical backgrounds in the joint angle estimation [22]. To make it more robust, the surgical manipulator

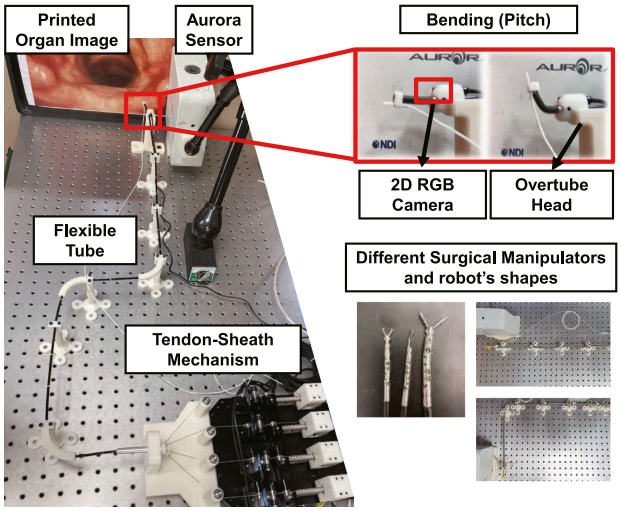

Fig. 1. **Experimental setup for evaluating ViO-Com with a flexible surgical robot.** Different size of surgical manipulators and the robot with variant sheath configurations have disparate cabling properties and hysteresis.

segmentation images used as the input for joint angle estimation were obtained by modifying CycleGAN [23]. The main concept of GAN is adversarial training between the generator (G) and the discriminator (D). The adversarial training aims D to be non-differentiated between the real image and the generated or fake image from G. To do so, G has to make a fake image as similar as the real image. In Fig. 2, G generates the binary image ($\hat{I}_{bi}$) without background from the input RGB image (I_{RGB}) using CycleGAN. CycleGAN is a domain transfer algorithm which uses two generator (G and F), and it has provided outstanding results in many applications [24], [25].

The loss function of the original CycleGAN was modified because camera images (RGB domain) should be accurately converted into segmented images (binary domain) in pixel units. For details, the L_1 loss between the pair of $\hat{I}_{bi}$ generated from the I_{RGB} and the real binary images (I_{realbi}) was added to the original loss given in Equation 1.

$$Loss = CycleGANloss + ||G(I_{RGB}) - I_{realbi}||_1. \quad (1)$$

We collected 5,040 RGB images (I_{RGB}, 84 cases of organ image from LapGyn4 dataset [26] $\times$ 60 cases of joint angle θ_a), and annotated the corresponding real binary images (I_{realbi}) with annotation tool [27]. The segmentation network was implemented using Tensorflow [28]. The ADAM Optimizer [29] with the learning rate $= 0.0001$, $\beta_1 = 0.9$, and $\beta_2 = 0.999$ was used for the optimization process. Xavier initialization [30] was used to initialize the weights of the network. The number of epochs was 30 with a single batch size for each training process.

C. Estimating Joint Angle of Surgical Manipulator using Siamese Convolutional Neural Network

Considering a real surgical robot application, we used a marker-less joint angle estimation scheme [19] with robust surgical manipulator segmentation. The concept is to find the most similar image $I_{vir}^{(i)}$ $(i = 1, 2, ..., m)$ from a pre-built database I_{vir} ($I_{vir}^{(i)} \in I_{vir}$) relative to the image $\hat{I}_{bi}$ obtained through GAN-based surgical manipulator segmentation. Herein, I_{vir} was obtained using the Gazebo simulator. The similarity between two images is defined as the Euclidean distance between the feature vectors f_{vir} and f_{bi}, which are the Siamese convolutional neural network (SCNN) outputs of the two images. Calculation of the distance between the feature vectors to search for the most similar image was performed using a k-d tree, a well-known and efficient searching algorithm.

We collected data to train the SCNN to build the joint angle estimator. The data were constructed using several paired data $(S^{(j)}, \hat{I}_{bi}^{(j)}, I_{vir}^{(j)})_{j=1}^{M}$, $M = 2 \times m \times \iota \times \nu$, $m = 61, \iota = 100, \nu = 3$. The range of θ_a $(= m)$ was determined based on an angle that is widely used in real surgeries [31]. The parameters ν and ι were set empirically based on the diversity of the data distribution. If $\hat{I}_{bi}^{(i)}$ and $I_{vir}^{(i)}$ represent the same joint angle, the label S is 1; otherwise, S is 0. Each image was named based on its representative joint angle θ_a in degree (e.g., 01,02,...,60.png), and θ_a was measured using an electromagnetic sensor called Aurora (Northern Digital Inc, Canada), which is commonly used in the medical robotics field.

The architectures of the SCNN, optimization function, and initialization method are identical to those described in [19]. During the training of the SCNN, the size of the input images ($\hat{I}_{bi}$, I_{vir}) was 128, and the batch size was 100.

Generally, the sampling rate of an endoscopic camera is less than 30 Hz, which is considerably lower than the sampling rate of the desired input signal (1 kHz). In addition, because the estimated joint angle $\hat{\theta}$ can oscillate unsteadily due to unexpected noise, we applied a Kalman filter to predict $\hat{\theta}$ in consideration of advantages in helping unstable sensors or estimators more accurate and stable by using a mathematical model information. The mathematical model and the structure of the proposed method are identical to those of the previous method [19], except that only one measurement is used in the proposed method.

D. Identifying Bouc-wen Hysteresis Model Parameters and Designing Feed-Forward Controller

1) Bouc-Wen hysteresis and its inverse model: The Bouc-Wen model has six hyperparameters that must be predefined before operating a system. The hyperparameters A, B, C, and n determine the shape and size of the hysteresis loop; α, and β are scale factors representing the ratio between $\hat{\theta}_b^{(k)}$, $\theta_{desired}^{(k)}$, and $h^{(k)}$. The symmetric Bouc–Wen model and its inverse model used in this work can be expressed as follows:

$$\hat{\theta}_b^{(k)} = \alpha\theta_{desired}^{(k)} + \beta h^{(k)}, \quad (2)$$

$$\dot{h}^{(k)} = A\dot{\theta}_{desired}^{(k)} - B|\dot{\theta}_{desired}^{(k)}||h|^{n-1}h - C\dot{\theta}_{desired}^{(k)}|h|^n, \quad (3)$$

$$\theta_c^{(k)} = \frac{1}{\alpha}(\theta_{desired}^{(k)} - \beta h^{(k)}), \quad (4)$$

where $\hat{\theta}_b^{(k)}$ is the estimated joint angle obtained from the Bouc-Wen model; $\theta_{desired}^{(k)}$ is a time-series desired input. The internal state $h^{(k)}$ is the solution of differential Equation 3. In order to apply the Bouc-Wen model into a feedforward controller, we

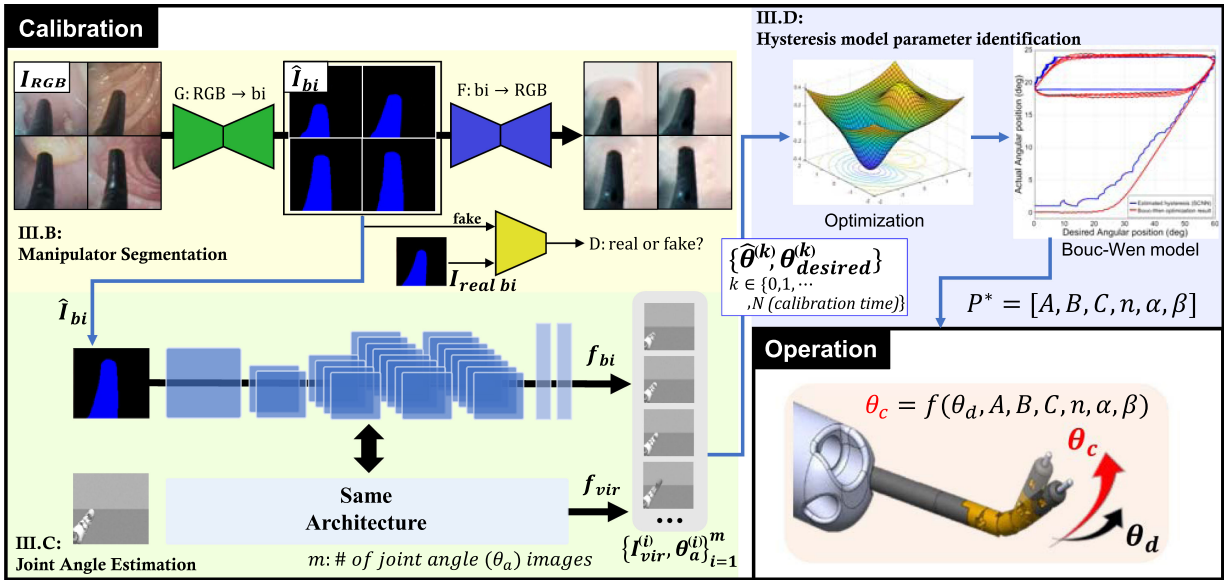

Fig. 2. **Pipeline of ViO-Com.** RGB organ image (I_{RGB}) acquired from an endoscopic camera is converted to the binary image ($\hat{I}_{bi}$) by using the modified CycleGAN. The SCNN extracted the features in the binary image and this feature is utilized to search the most similar virtual image to the binary image in the pre-built virtual image dataset (I_{vir}). During the calibration phase, the sinusoidal periodic signal is given to the surgical manipulator so the sequence data in calibration period ($k \in 0, 1, \ldots, N$) including the desired angles ($\theta^{(k)}_{desired}$) and the estimated angles ($\hat{\theta}^{(k)}$) is obtained simultaneously. With this data, the BFGS optimization method identifies the Bouc-Wen model parameters (non-optimized, P) and the feed-forward compensation using the Bouc-Wen model with optimized parameters (P^*) is finally available to apply to a surgical manipulator.

optimized the six parameters $P^* = [A, B, C, n, \alpha, \beta]$ via our vision-based joint angle estimation. The compensated input $\theta^{(k)}_c$ can be calculated and implemented in a cable-driven robot after the calibration process.

2) Bouc-Wen hysteresis model parameter identification: In the robot calibration phase before the operation, the unknown model parameters P of the proposed system must be identified, meaning that accuracy and speed of the optimization should be considered for making the use of practical applications. In parameter optimization, the fitness function given by Equation 5 is used.

$$\min_P \frac{1}{N} \sum_{k=1}^{N} (\hat{\theta}^{(k)} - \hat{\theta}^{(k)}_b)^2, \tag{5}$$

where N is total number of samples acquired during calibration, $\hat{\theta}^{(k)}$ the estimated joint angle obtained using the vision-based joint angle estimator, and $\hat{\theta}^{(k)}_b$ output of the Bouc-Wen model.

We suggest the use of the Broyden Fletcher Goldfarb Shanno (BFGS) algorithm [18, 19] that typically requires fewer function calls instead of the simplex algorithm (e.g., Powell and Nelder–Mead) to identify the Bouc–Wen model parameters for accurately describing the hysteresis properties. This approach eliminates the need for hyperparameter tuning during parameter optimization by using the SciPy package [32], and it is often faster than the gradient descent approach when applied to nonlinear parameter estimation. To provide a more grounded suggestion, we evaluated nine different optimization algorithms, including BFGS, as described in Section IV.

IV. EXPERIMENT

A. Optimization Comparison for Bouc-Wen Model

The first experiment in Section V-A aimed to find the most adequate optimization algorithm for identifying the Bouc-Wen model parameters in terms of the accuracy and the time cost. Mean square error (MSE) was used as an accuracy indicator. If the system fails to optimize during operation, it will bring critical adverse effect due to unexpected movement of the manipulator. So we predefined the optimization success when the MSE of the algorithm gets less than 3°, and the time cost was recorded under the satisfied condition. Meanwhile, the succeed rate was compared.

Nine traditional optimization algorithms, namely genetic algorithm (GA); particle swarm algorithm (PSO); and several optimization methods included in the SciPy package, such as Nelder–Mead, Powell, CG, BFGS, TNC, COBYLA, and SLSQP, were compared and evaluated [32]. We acquired 18 different hysteresis cases by changing the sheath configuration (a flexible tube) of the robot from 0° to 255° in steps of 15°. Because the optimization performance is strongly affected by the initial parameter settings, the initial parameters were arbitrarily selected to ensure a fair assessment. Based on our empirical knowledge, the lower and upper bounds of the initial parameters at 0° and 255°, respectively, were determined beforehand by referring to the optimized parameters identified using a GA available in the MATLAB global optimization toolbox.

B. Quantitative Evaluation of ViO-Com

The second experiment in Section V-B was conducted to validate the ViO-Com. In order to compose multiplex

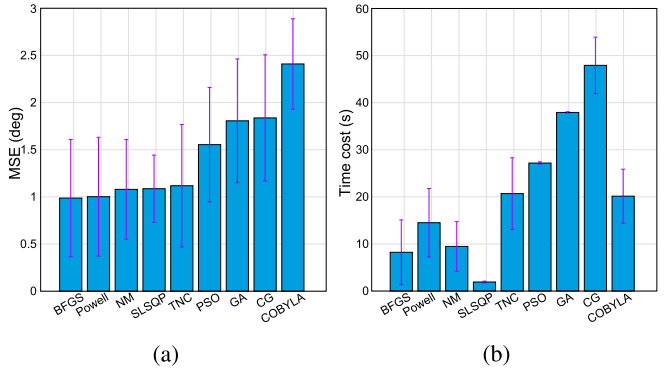

Fig. 3. **Comparison results between optimization algorithms.** (*mean*±*sd*) (a) Accuracy (b) Time cost.

circumstance with unknown variant prior hysteresis, We changed the hysteresis condition from case one to case four by deforming a flexible tube and altering the diameter of the kinematic parameter, which is similar to switching to another surgical manipulator. For investigating the influence according to the change of the movement speed of the manipulator, Three different periodic motions (with the same amplitude and different frequencies) and a non-periodic motion (a combination of three signals) were applied. Root mean square error (RMSE) between the desired input θ_d and the actual joint angle θ_a was used as an evaluation criterion. Five trials were carried out per individual case.

To verify the feasibility of ViO-Com in various hysteresis cases (Cases 1–4) that cannot be measured during real surgical operation, we have benchmarked ViO-Com against two baselines: (1) Without compensation (Without Com), (2) Vision-based feedback compensation (Feedback Com)[21].

In each condition of the experiment, Bouc-Wen model parameters of ViO-Com was optimized respectively by the joint angle estimator with GAN-based surgical manipulator segmentation. The accuracy of the joint angle estimator used in this evaluation is less than 3°, computed as the root mean square error (RMSE) between the $\hat{\theta}$ and θ_a. Sinusoidal input (30sinωt+30° and frequency of 0.1592 Hz) was provided as the calibration signal in all of the cases. Fig. 4. presents the sample results of each of the partial methods that were executed in the ViO-Com process. The GAN-based surgical tool segmentation generated a similar output image by extracting an only the surgical manipulator from a variety of surgical backgrounds. The estimation performance was similar to that obtained in our study [21], which was conducted under unsophisticated conditions.

V. RESULT AND DISCUSSION

A. Comparison and Analysis of Optimization Methods

In our implementation, BFGS was selected due to the best accuracy and time cost. Fig. 3 indicates the optimization ability between nine algorithms for Bouc-Wen model. Since we predefined the optimization success condition as 3°under the MSE, all of the MSEs of algorithms are under 3°. SLSQP seems the best algorithm owing to its fastest convergence speed, however, it only recorded 3 successes among 18 trials; whereas

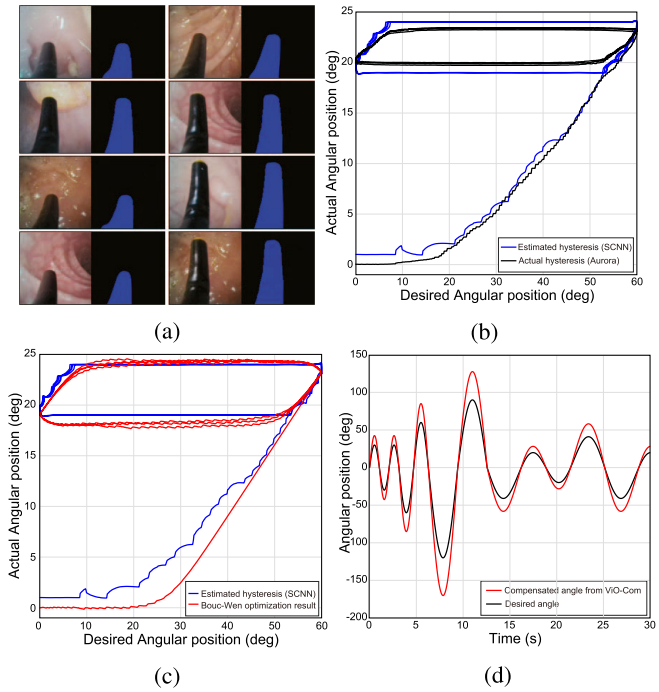

Fig. 4. **Sample result of element in ViO-Com flow.** (a) GAN-based surgical manipulator segmentation. (b) Estimation of the joint angle of the manipulator. (c) Identifying Bouc-Wen model parameters using ViO-Com (d) Expected compensation input given non-periodic signal.

BFGS recorded 17 successes in the same trials. Powell also got 17 successes and similar MSE with BFGS, the time cost difference makes Powell not be chosen. Therefore, after the calibration, ViO-Com elicits Bouc-Wen model parameters using BFGS which well reflects hysteresis characteristics with high convergence speed.

BFGS has a comparatively low computational time, because it requires fewer function calls than simplex algorithms, such as Powell and NM, and does not need a matrix inversion. Although evolutionary optimization methods such as GA and PSO have been proven to be efficient for global optimization problems, their performance lags behind the performance of simplex methods. Simplex optimization algorithms are highly accurate and fast when compared to other methods when the objective function and constraints are linear functions of the variables. However, because the identification of the Bouc–Wen model parameters is a considerably nonlinear problem, it is necessary to simplify or linearize the problem to make use of the specificity of the simplex method. We expect that by determining the initial parameter values based on our heuristic knowledge, which use bounded parameters of smallest and biggest hysteresis, might positively influence the process of redefining optimization problems to simplify them.

B. Verifying ViO-Com in terms of Compensating Hysteresis

We have summarized the performance of ViO-Com in Table I. ViO-Com shows an average performance increase of more than 67% in four cases compared to the without-compensation scenario. In addition, the performance of ViO-Com is superior to that of vision-based feedback compensation in all cases, except

TABLE I

HYSTERESIS COMPENSATION PERFORMANCE BENCHMARK. EACH CASE HAS DIFFERENT PRIOR HYSTERESIS. PERIODIC MOTIONS (P) WITH DIFFERENT FREQUENCY AND NON-PERIODIC MOTION (N-P) ARE GIVEN AS AN INPUT SIGNAL. ALL RESULTS MEAN RMSE(°) BETWEEN θ_d AND θ_a.

Hysteresis	**Case 1**				**Case 2**				**Case 3**				**Case 4**			
Signal (w)	P (0.25)	P (0.5)	P (1)	N-P (1)	P (0.25)	P (0.5)	P (1)	N-P (1)	P (0.25)	P (0.5)	P (1)	N-P (1)	P (0.25)	P (0.5)	P (1)	N-P (1)
Without Com	21.37	19.38	22.66	18.92	18.08	17.98	18.66	15.07	16.66	16.50	17.08	8.35	13.53	14.96	14.08	13.17
Average	**20.58**				**17.45**				**14.64**				**13.93**			
Feedback Com	6.46 ±0.40	6.34 ±0.88	9.66 ±0.46	8.40 ±0.14	6.09 ±0.06	7.66 ±0.09	8.53 ±0.11	8.03 ±0.18	4.18 ±0.16	5.22 ±0.07	7.11 ±0.04	6.44 ±0.16	3.37 ±0.06	3.82 ±0.06	5.21 ±0.06	5.40 ±0.10
Average	**7.72**				**7.58**				**5.74**				**4.45**			
ViO-Com	6.13 ±0.51	7.01 ±0.56	6.55 ±0.27	5.99 ±0.38	3.96 ±0.05	4.02 ±0.14	4.51 ±0.10	3.96 ±0.18	4.92 ±1.27	4.27 ±1.21	4.77 ±0.82	6.45 ±0.55	5.61 ±0.70	4.78 ±0.30	4.78 ±1.26	6.48 ±0.52
Average	**6.42**				**4.09**				**5.10**				**5.41**			

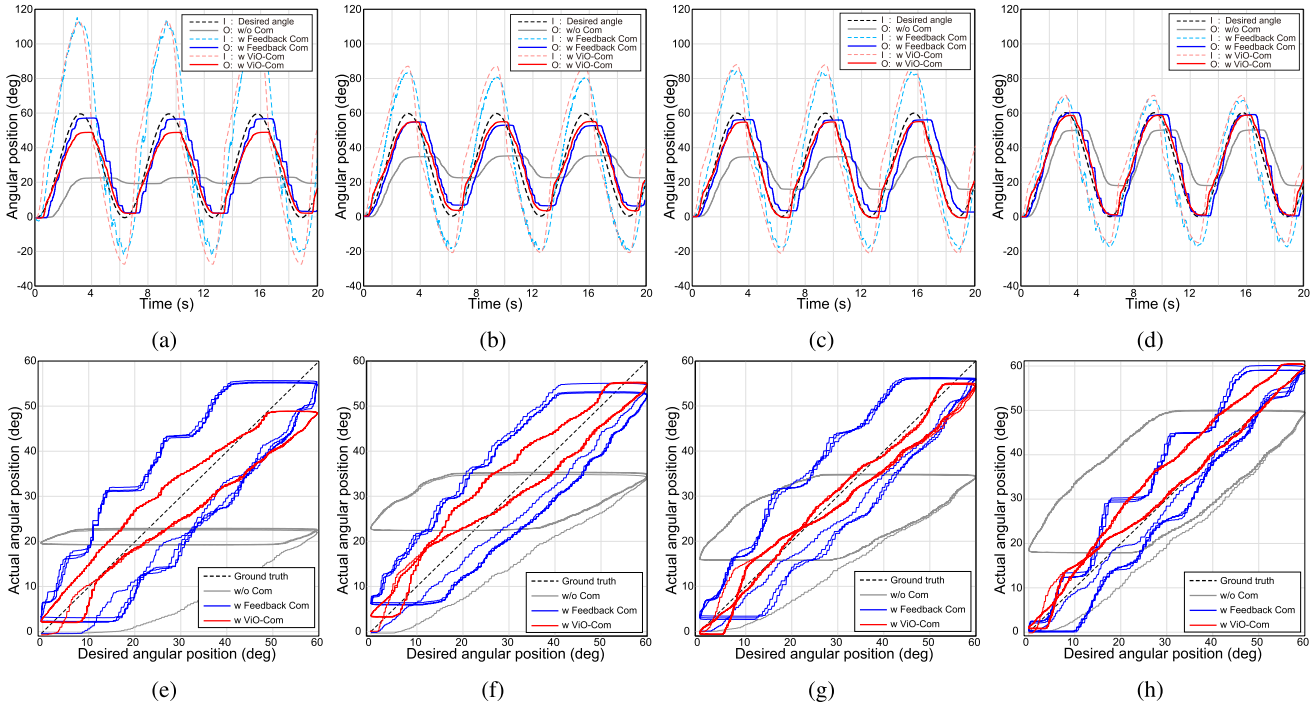

Fig. 5. **Hysteresis compensation result of ViO-Com in comparison with two baselines (Without Com and With Feedback Com).** Figure (a) to (d) indicate the tracking performance for periodic motion in accordance passing of time (Input and output signals are described as a dotted line and a solid line, respectively) and figure (e) to (h) show the comparison of hysteresis compensation performance of each methods. The figures in same column are result in the same experiment condition (Case1 - Case4). The size of prior hysteresis become smaller from case1 to case4.

case 4. In the case with small hysteresis, the error between the target and the current positions decreases relatively quickly, even when using only low control parameter values, meaning that the section affected by the slow vision-based feedback provided using a low camera sampling rate (30 Hz) might not strongly influence the control performance. We believe that for this reason, the vision-based feedback method performed better than ViO-Com in the last case. Unlike the vision-based feedback compensation scheme that is affected by frequency changes and magnitude of hysteresis, the performance of the proposed method is almost unaffected by changes in frequency. This suggests that ViO-Com can maintain the desired surgical performance, regardless of individual users' personality traits (e.g., master's operation speed). According to Fig. 5, the results obtained using ViO-Com are significantly more stable than those obtained using the vision-based method. Because ViO-Com uses constant parameter values in feedforward compensation, it enables keep safe movement regardless of changes in external conditions (e.g., surgical smoke, debris, unstable sensor or estimator output). The result of ViO-Com seems to deviate to the left of the plot in the section where the desired angle $\theta_{desired}$ is small. This is because the condensed force accumulated while initially stationary due to static friction acted momentarily. Fig. 6 displays the hysteresis performance results of ViO-Com given a non-periodic signal that is similar to the actual master device input. The results are not substantially different from those obtained by providing a periodic signal.

ViO-Com is proposed in view of practical circumstances, and the calibration phase for optimizing the Bouc–Wen model parameters by using an endoscopic camera lasts less than 1 min (Input signal: 20sec, Optimization process: 10 20 sec). Considering the high cost of external sensors (e.g., electromagnetic sensor, FBG sensor) and the uncertainty of robot shape, ViO-Com can be regarded a realistic solution to compensate for the hysteresis of

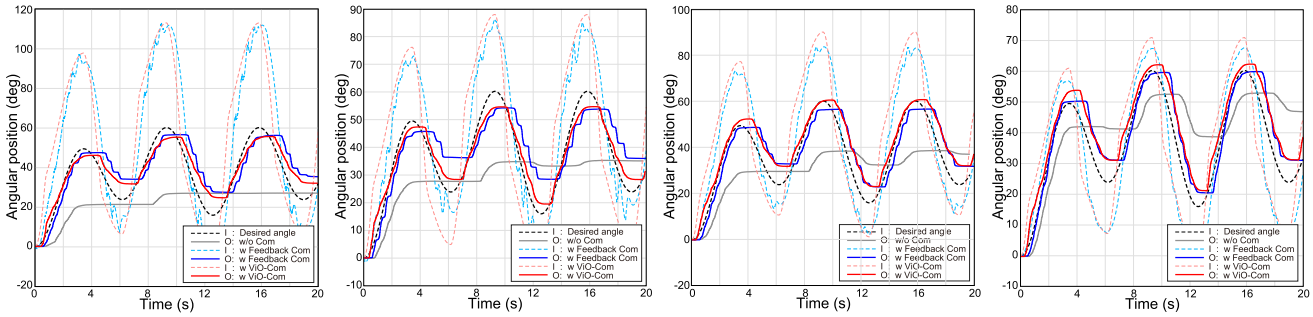

Fig. 6. **Tracking Performance Result of ViO-Com.** Each figure indicates comparison result of ViO-Com and two baselines given non-periodic signal. Input and output signals are represented as same as Fig. 3.

flexible cable-driven surgical robots in constrained conditions, where arbitrary unknown robot shapes and unexpected surgical situations may be encountered. The experimental compensation results indicate that ViO-Com facilitates the smooth operation of a flexible cable-driven robot even inside a colon with a decently curved section. Additionally, ViO-Com can be easily implemented with a simple feed-forward controller.

Although we demonstrated the ViO-Com in only bending joint, it can easily expand to two bending joint because ViO-Com does not require a large amount of data for applying this to other bending joint. Moreover, we assumed that the change of robot shape is the most influential factor in hysteresis compared to other factors if initial wire elongation is not large, so applying the same optimized parameter to two bending joints looks reasonable approach and we present this result as a video. In this work, we focused on reducing hysteresis of the bending joint of the manipulator because it can considerably increase surgical performance [4]. However, in surgical scenarios where the overtube changes in real time, the performance of ViO-Com may be limited. This limitation can be overcome by combining the proposed method with an online parameter estimation or update method, such as the unscented Kalman filter. Evidently, the performance of the proposed method might also deteriorate when the appearance of the tool change and occlusion exist. Although it is hard to apply the same trained model to different surgical robot, ViO-Com is robust against the variation of sheath length and end-tips since it uses binary image focusing on 2D shape of tool body. Also, ViO-Com is performed before surgical operation, and therefore, we assumed that the level of occlusion is low.

VI. CONCLUSION

We presented a novel hysteresis compensation pipeline called ViO-Com that improves the control accuracy of a cable-driven surgical robot without requiring the use prior hysteresis knowledge as a utilitarian solution. ViO-Com uses a Bouc–Wen-model-based feedforward controller that is optimized by utilizing only a two-dimensional camera image. Because ViO-Com does not rely on an estimator or sensors during operation, it cannot be negatively affected by dynamic surgical environments, meaning that it can maintain stable manipulator motion. The validation results of ViO-Com shows that it enhances the control accuracy of a surgical manipulator under various hysteresis condition. Moreover, its performance is superior to that of vision-based feedback compensation.

In future works, we will investigate how to increase the accuracy and robustness of joint angle estimation, maintain control accuracy during surgical operation, and apply ViO-Com to two surgical arms of K-FLEX for verifying its performance by conducting ex-vivo surgical tasks.

REFERENCES

[1] M. Hwang and D.-S. Kwon, "K-FLEX: a flexible robotic platform for scar-free endoscopic surgery," *Int. J. Med. Robot. Comput. Assist. Surg.*, vol. 16, no. 2, Apr. 2020, Art. no. e2078.

[2] P. J. Schuler *et al.*, "Hybrid procedure for total laryngectomy with a flexible robot-assisted surgical system," *Int. J. Med. Robot. Comput. Assist. Surg.*, vol. 13, no. 2, Jun. 2017, Art. no. e1749, doi: 10.1002/rcs.1749.

[3] D. B. Camarillo, C. F. Milne, C. R. Carlson, M. R. Zinn, and J. K. Salisbury, "Mechanics modeling of tendon-driven continuum manipulators," *IEEE Trans. Robot.*, vol. 24, no. 6, pp. 1262–1273, Dec. 2008.

[4] H. Kim, M. Hwang, J. Kim, J. M. You, C.-S. Lim, and D.-S. Kwon, "Effect of backlash hysteresis of surgical tool bending joints on task performance in teleoperated flexible endoscopic robot," *Int. J. Med. Robot. Comput. Assist. Surg.*, vol. 16, no. 1, 2020, Art. no. e2047.

[5] V. Hassani and T. Tjahjowidodo, "Structural response investigation of a triangular-based piezoelectric drive mechanism to hysteresis effect of the piezoelectric actuator," *Mech. Syst. Signal Process.*, vol. 36, no. 1, pp. 210–223, 2013.

[6] T. Do, T. Tjahjowidodo, M. Lau, T. Yamamoto, and S. Phee, "Hysteresis modeling and position control of tendon-sheath mechanism in flexible endoscopic systems," *Mechatronics*, vol. 24, no. 1, pp. 12–22, 2014.

[7] T. Do, T. Tjahjowidodo, M. Lau, and S. Phee, "Adaptive control for enhancing tracking performances of flexible tendon-sheath mechanism in natural orifice transluminal endoscopic surgery," *Mechatronics*, vol. 28, pp. 67–78, 2015.

[8] Y. Jung and J. Bae, "Torque control of a double tendon-sheath actuation mechanism in varying sheath configuration," in *Proc. IEEE Int. Conf. Adv. Intell. Mechatronics*, 2017, pp. 1352–1356.

[9] A. Rossi, A. Trevisani, and V. Zanotto, "A telerobotic haptic system for minimally invasive stereotactic neurosurgery," *Int. J. Med. Robot. Comput. Assist. Surg.*, vol. 1, no. 2, pp. 64–75, 2005.

[10] R. A. Porto, F. Nageotte, P. Zanne, and M. de Mathelin, "Position control of medical cable-driven flexible instruments by combining machine learning and kinematic analysis," in *Proc. Int. Conf. Robot. Automat.*, 2019, pp. 7913–7919.

[11] D. Wu, Y. Zhang, M. Ourak, K. Niu, J. Dankelman, and E. V. Poorten, "Hysteresis modeling of robotic catheters based on long short-term memory network for improved environment reconstruction," *IEEE Robot. Automat. Lett.*, vol. 6, no. 2, pp. 2106–2113, Apr. 2021.

[12] D.-H. Lee, Y.-H. Kim, J. Collins, A. Kapoor, D.-S. Kwon, and T. Mansi, "Non-linear hysteresis compensation of a tendon sheath driven robotic manipulator using motor current," *IEEE Robot. Automat. Lett.*, vol. 6, no. 2, pp. 1224–1231, Apr. 2021.

[13] T. Reichl, J. Gardiazabal, and N. Navab, "Electromagnetic servoing-A new tracking paradigm," *IEEE Trans. Med. Imag.*, vol. 32, no. 8, pp. 1526–1535, Aug. 2013.
[14] L. Zhang, M. Ye, P.-L. Chan, and G.-Z. Yang, "Real-time surgical tool tracking and pose estimation using a hybrid cylindrical marker," *Int. J. Comput. Assist. Radiol. Surg.*, vol. 12, no. 6, pp. 921–930, 2017.
[15] P. Cabras, F. Nageotte, P. Zanne, and C. Doignon, "An adaptive and fully automatic method for estimating the 3D position of bendable instruments using endoscopic images," *Int. J. Med. Robot. Comput. Assist. Surg.*, vol. 13, no. 4, 2017, Art. no. e1812.
[16] M. Allan, S. Ourselin, D. J. Hawkes, J. D. Kelly, and D. Stoyanov, "3-D pose estimation of articulated instruments in robotic minimally invasive surgery," *IEEE Trans. Med. Imag.*, vol. 37, no. 5, pp. 1204–1213, May 2018.
[17] D. Baek, J.-H. Seo, J. Kim, and D.-S. Kwon, "Image-based hysteresis compensator for a flexible endoscopic surgery robot," in *Proc. 16th Int. Conf. Ubiquitous Robots*, 2019, pp. 299–305.
[18] D. Baek, J.-H. Seo, J. Kim, and D.-S. Kwon, "Hysteresis compensator with learning-based pose estimation for a flexible endoscopic surgery robot," in *Proc. IEEE/RSJ Int. Conf. Intell. Robots Syst.*, 2019, pp. 2983–2989.
[19] T. Poignonec, P. Zanne, B. Rosa, and F. Nageotte, "Towards in situ backlash estimation of continuum robots using an endoscopic camera," *IEEE Robot. Automat. Lett.*, vol. 5, no. 3, pp. 4788–4795, Jul. 2020.
[20] S. Paradis *et al.*, "Intermittent visual servoing: Efficiently learning policies robust to instrument changes for high-precision surgical manipulation," in *Proc. IEEE Int. Conf. Robot. Automat.*, 2020, pp. 7166–7173.
[21] D. Baek, J.-H. Seo, J. Kim, and D.-S. Kwon, "Hysteresis compensator with learning-based hybrid joint angle estimation for flexible surgery robots," *IEEE Robot. Automat. Lett.*, vol. 5, no. 4, pp. 6837–6844, Oct. 2020.
[22] C.-C. Wong, L.-Y. Yeh, C.-C. Liu, C.-Y. Tsai, and H. Aoyama, "Manipulation planning for object re-orientation based on semantic segmentation keypoint detection," *Sensors*, vol. 21, no. 7, p. 2280, 2021.
[23] J.-Y. Zhu, T. Park, P. Isola, and A. A. Efros, "Unpaired image-to-image translation using cycle-consistent adversarial networks," in *Proc. IEEE Int. Conf. Comput. Vis.*, 2017, pp. 2223–2232.
[24] Z. Wang, Q. She, and T. E. Ward, "Generative adversarial networks in computer vision: A survey and taxonomy," *ACM Comput. Surv.*, vol. 54, no. 2, pp. 1–38, 2021.
[25] Y.-H. Nho, S. Ryu, and D.-S. Kwon, "UI-GAN: Generative adversarial network-based anomaly detection using user initial information for wearable devices," *IEEE Sensors J.*, vol. 21, no. 8, pp. 9949–9958, Apr. 2021.
[26] A. Leibetseder *et al.*, "LapGyn4: A dataset for 4 automatic content analysis problems in the domain of laparoscopic gynecology," in *Proc. 9th ACM Multimedia Syst. Conf.*, 2018, pp. 357–362.
[27] K. Wada, "Labelme: Image polygonal annotation with Python," 2016. [Online]. Available: https://github.com/wkentaro/labelme
[28] M. Abadi *et al.*, "TensorFlow: A system for large-scale machine learning," in *Proc. 12th USENIX Symp. Operating Syst. Des. Implementation*, 2016, pp. 265–283.
[29] D. P. Kingma and J. Ba, "Adam: A method for stochastic optimization," 2014, *arXiv:1412.6980*.
[30] X. Glorot and Y. Bengio, "Understanding the difficulty of training deep feedforward neural networks," in *Proc. 13th Int. Conf. Artif. Intell. Statist.*, 2010, pp. 249–256.
[31] S. Soni, K. Singh, S. Verma, D. Pankaj, and A. Kumar, "Kinematic and dynamic analysis of a surgical tool manipulator towards robotic surgery," in *Proc. 1st Int., 16th Nat. Conf. Mach. Mechanisms*, 2013, pp. 987–991.
[32] P. Virtanen *et al.*, "SciPy 1.0: Fundamental algorithms for scientific computing in Python," *Nature Methods*, vol. 17, no. 3, pp. 261–272, 2020.